Physicochemical Characterization of Ferrocifen Lipid Nanocapsules: Customized Drug Delivery Systems Guided by the Molecular Structure

Pierre Idlas, Elise Lepeltier, Guillaume Bastiat, Pascal Pigeon, Michael Mcglinchey, Nolwenn Lautram, Anne Vessieres, Gérard Jaouen, Catherine Passirani

Physico-chemical characterization of ferrocifen lipid nanocapsules: customized drug delivery systems guided by the molecular structure

Pierre Idlas[1], Elise Lepeltier[1,*], Guillaume Bastiat[1], Pascal Pigeon[2,3], Michael J. McGlinchey[4], Nolwenn Lautram[1], Anne Vessières[2], Gerard Jaouen[2,3] and Catherine Passirani[1]

[1] Micro et Nanomédecines Translationnelles, MINT, UNIV Angers, INSERM 1066, CNRS 6021, Angers, France`

[2] Sorbonne Université, CNRS, Institut Parisien de Chimie Moléculaire (IPCM), 75005 Paris, France

[3] Chimie Paris Tech, PSL University, 75005 Paris, France

[4] UCD School of Chemistry, University College Dublin, Belfield, Dublin 4, Ireland

* Corresponding author: elise.lepeltier@univ-angers.fr

ABSTRACT

Ferrocifens, lipophilic organometallic complexes, are comprised of a biologically active redox motif [ferrocenyl-ene-*p*-phenol] conferring on this family very interesting cytotoxic properties. However, because of their highly lipophilic nature, a formulation stage is required before being administered *in vivo*. In recent decades, ferrocifen lipid nanocapsules (LNCs) have been successfully formulated and have demonstrated anticancer properties on multidrug-resistant cancers on several mice and rat models (glioblastoma, breast cancer, metastatic melanoma). A recent family of ferrocifens (succinimidoalkyl-ferrociphenols, including **P722**) appears to be the most efficacious on several resistant cancer cell lines, with IC_{50} values in the nanomolar range together with promising *in vivo* results on murine ovarian cancer models. As LNCs are composed of an oily core (caprylic/capric triglycerides), modulation of the succinimido-ferrociphenol lipophilicity could be a valuable approach towards improving the drug loading in LNCs. As drug loading of the diphenol **P722** in LNCs was low, it was structurally modified to increase its lipophilicity and thereby the payload in LNCs. Chemical modification led to a series of five succinimido-ferrocifens. Results confirmed that these slight structural modifications led to increased drug loading in LNCs for all ferrocifens, with no reduction of their cytotoxicity on the SKOV3 ovarian cancer cell line. Interestingly, encapsulation of two of the ferrocifens, the diester **P769** and the monophenolic ester **(*E*)-P998** led to the formation of a gel. This was unprecedented behaviour, a phenomenon that could be rationalized in terms of the positioning of ferrocifens in LNCs as shown by the decrease of interfacial tension measurements at the water/oil interface. Moreover, these results highlighted the importance to obtaining a gel of this particular motif, in which the acetylated phenolic ring and the succinimidoalkyl moieties are mutually *cis* relative to the central double bond. Promising perspectives to use these ferrocifen-loaded LNCs to treat glioblastoma could be readily envisaged by local application of the gel in the cavity after tumour resection.

INTRODUCTION

Nanomedicine is a very active multidisciplinary field with large investments, internationally notably recognized since the success of the Covid-19 vaccination nanoplatform developed by Pfizer/BioNTech and Moderna. Since the 1960s, one of the main objectives of the field has been to develop new therapeutic strategies to treat cancers,[1] and much progress has been made towards increasing the amount of conventional chemotherapeutic agent reaching the cancer site, in avoiding healthy tissues, by the use of vectors such as liposomes[2], polymeric nanocapsules[3–7] and lipid-prodrug nanoparticles[8]. However, resistance phenomena to classic chemotherapies are too often observed, hence the need to bring to market new small active molecules to overcome this problem. In the late 1980s, a new class of bioorganometallic molecules was developed,[9,10] among which complexes containing a transition metal (iron, ruthenium, osmium, rhodium) were tested, and those in the ferrocifen family were found to be the most promising.[11] Ferrocifens, are lipophilic biologically active organometallic complexes, containing the [ferrocenyl-ene-*p*-phenol] redox motif. The earliest ferrocifen, (**P15** or Fc-OH-Tam), in which the phenyl substituent adjacent to the ethyl in hydroxytamoxifen was replaced by a ferrocenyl unit, showed an anti-estrogenic effect on the estrogen receptor-positive (ER+) breast cancer line MCF-7 and also a cytotoxic effect on the ER- triple negative breast cancer MDA-MB231.[12,13] The cytotoxic behavior was found to be related to the unique redox properties of this molecule. Indeed, a number of studies highlighted the role of the reversible Fe(II)/Fe(III) oxidation of the ferrocenyl moiety, leading to formation of an electrophilic quinone methide (QM) and the production of reactive oxygen species (ROS), inducing senescence and/or apoptosis.[14,15] Subsequent structure-activity relationship studies of structurally modified ferrocifens have allowed the elucidation of their mechanisms of action.[11] Among the multitude of compounds containing hydroxyalkyl or alkylimido substituents, the propylsuccinimido-ferrocifens, in particular the diphenol **P722** (Figure 1), showed an increase in cytotoxicity on several cancer cell lines compared to previously studied ferrocifens. This dramatic improvement was rationalized in terms of a lone pair-π interaction between a carbonyl group of the imide and the plane of the neighboring aromatic QM ring leading to enhanced long-term stability.[16,17]

However, as for most anticancer drug candidates, ferrocifen compounds are poorly soluble in water, requiring a formulation stage before *in vivo* administration. For two decades, lipid nanocapsules (LNCs) have demonstrated their ability to successfully encapsulate lipophilic drugs such as paclitaxel and ferrocifens.[18–21] LNCs are obtained by a low-energy emulsification method based on a phase-inversion process.[22] They are composed of a liquid oily core and a polyethylene glycol hydroxystearate surfactant shell. Recent studies have highlighted the successful encapsulation of the diphenol **P722** in LNCs, with promising *in vivo* results on metastatic melanoma, glioblastoma and epithelial ovarian cancer.[23–25] However, compared to other ferrocifens, drug loading of this compound in LNCs remains particularly weak.

The aim of this study was thus to modify the chemical structure of the diphenol **P722**, to obtain succinimido-ferrocifens with higher lipophilicity and thereby improve the payload in LNCs. **P722** was structurally modified leading to five ferrocifens: the diester **P769**, the monophenols **(*E*)** and **(*Z*)-P849**, and the monophenolic esters **(*E*)** and **(*Z*)-P998** (Figure 1). Of particular interest was the observation of unprecedented gel formation for **P769** and **(*E*)-P998**. Viscoelastic properties of the obtained ferrocifen-LNC gel were measured, depending on ferrocifen and particle concentrations. To understand gel formation, tensiometry measurements and the kinetics of LNC destabilization were studied. Finally, cell viability experiments on the ovarian cancer cell line SKOV3 were performed to determine whether chemical modifications on **P722** hampered its cytotoxic efficacy.

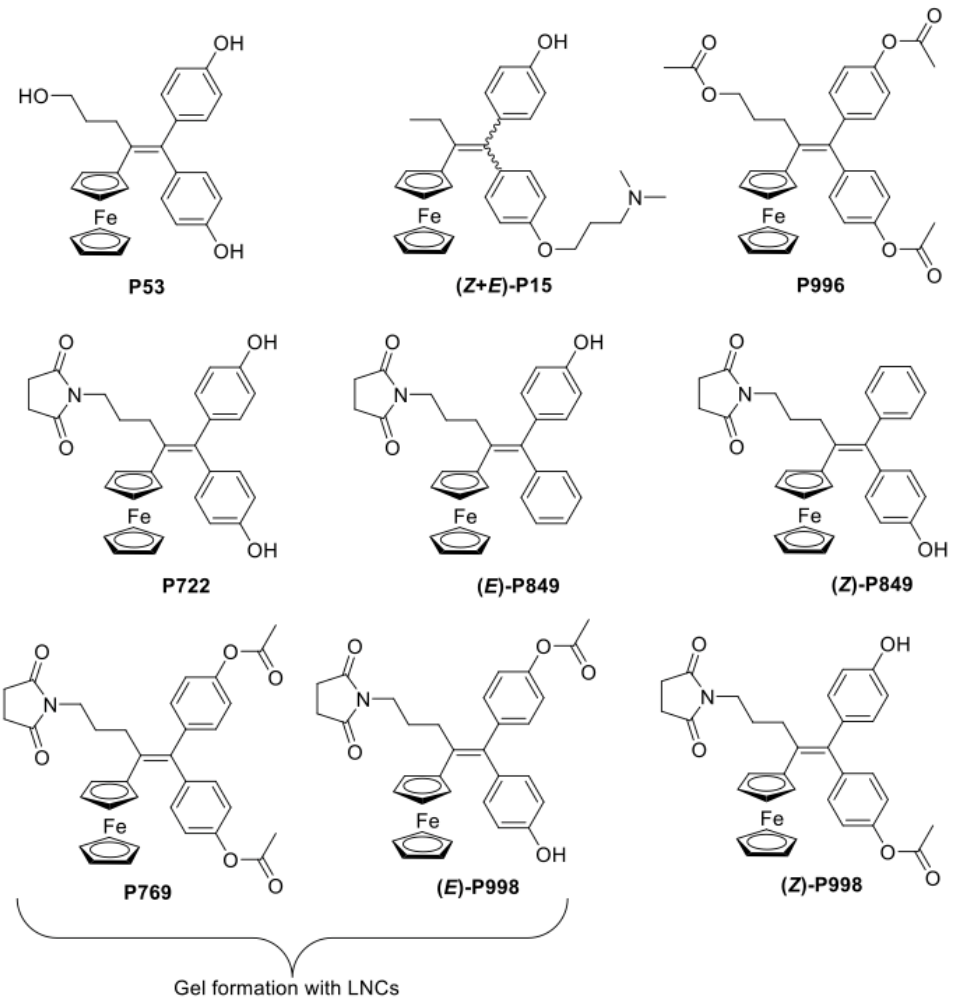

Figure 1: Molecular structures of the succinimido-ferrocifens under study and of earliest ferrocifens (**P15**[26]and **P53**[25]).

EXPERIMENTAL SECTION

Materials. All components of conventional blank LNCs are FDA-approved for parenteral administration. Macrogol 15 hydroxystearate (Kolliphor® HS 15) was purchased from BASF (Germany). Phosphatidylcholine from soybean (Lipoïd S 100) was provided by Lipoïd GmbH (Germany) and caprylic/capric triglycerides (Labrafac® WL 1349) were supplied by Gattefosse (France). Ultra-pure water (UPW) was obtained from a Millipore filtration system. All other reagents or solvents used (acetonitrile, methanol, dimethyl sulfoxide DMSO) for chromatography were of analytical grade. Ferrocifens **P722**,[16] **P849**,[17] and **P769**[35] were synthesized as described previously. Esterase from porcine liver was purchased from Merck (SigmaAldrich, Germany). Starting materials for the synthesis of **P998** were obtained commercially from Sigma–Aldrich or Alfa Aesar France. Thin layer chromatography was performed on silica gel 60 GF_{254}. IR spectra were obtained on a FT/IR-4100 JASCO 180 spectrometer. ^{1}H and ^{13}C NMR spectra were acquired on Bruker 300 or 400 MHz spectrometers. High-resolution mass spectra (HRMS) were acquired in the "Institut Parisien de Chimie Moléculaire (IPCM – UMR 8232)" at Sorbonne Université, Paris.

Synthesis of P998: (*Z*+*E*)-*N*-{4-ferrocenyl-5-(4-acetoxyphenyl)-5-(4-hydroxyphenyl)-pent-4-enyl}succinimide.

Acetic anhydride (0.325 g, 0.3 mL, 3.2 mmol) was added dropwise to a solution of **P722** (1.004 g, 1.88 mmol) and pyridine (0.593 g, 0.61 mL, 7.5 mmol) in dry THF (40 mL) at RT, then the reaction mixture was stirred for 5 h. The solution was then poured into water (400 mL). Concentrated hydrochloric acid (1 mL) was added under stirring, and the mixture was extracted twice with dichloromethane (400 mL). The combination of organic layers was dried over magnesium sulfate and concentrated under reduced pressure. Flash chromatography of the residue with a 2/1 solution of cyclohexane/ethyl acetate as the eluent was carried out. Since the *E* isomer (first out of the column) was not very well separated from by-product **P769** and the *Z* isomer was not very well separated from the remaining **P722**, a special technique had to be used: impure isomers were allowed to isomerize overnight in their eluent, the other appearing isomers being easily separated, being in an area without polluting compounds. Flash chromatography was repeated several times to increase the yield. Unfortunately, rapid isomerization gave *E* and *Z* isomers containing a certain quantity of others isomers, even during recrystallization from ethyl acetate/cyclohexane at -30°C, that furnished pure **P998** as an orange solid in an overall (*Z*+*E*) yield around 30-40 % (this yield is very dependent on the number of times the flash chromatography was repeated). ^{1}H NMR of *E* isomer (acetone-d_6): δ (ppm): 1.68-1.83 (m, 2H, CH_2), 2.26 (s, 3H, CH_3), 2.49-2.62 (m, 6H, succinimide + CH_2-C=C), 3.36 (t, *J* = 6.7 Hz, 2H, CH_2N), 3.93 (t, *J* = 1.9 Hz, 2H, C_5H_4), 4.09 (t, *J* = 1.9 Hz, 2H, C_5H_4), 4.13 (s, 5H, Cp), 6.73 (d, *J* = 8.6 Hz, 2H, C_6H_4), 6.90 (d, *J* = 8.6 Hz, 2H, C_6H_4), 7.09 (d, *J* = 8.6 Hz, 2H, C_6H_4), 7.22 (d, *J* = 8.6 Hz, 2H, C_6H_4). ^{1}H NMR of *Z* isomer (acetone-d_6): δ (ppm): 1.68-1.83 (m, 2H, CH_2), 2.23 (s, 3H, CH_3), 2.49-2.62 (m, 6H, succinimide + CH_2-C=C), 3.36 (t, *J* = 6.7 Hz, 2H, CH_2N), 3.89 (t, *J* = 1.9 Hz, 2H, C_5H_4), 4.09 (t, *J* = 1.9 Hz, 2H, C_5H_4), 4.13 (s, 5H, Cp), 6.83 (d, *J* = 8.6 Hz, 2H, C_6H_4), 6.97 (d, *J* = 8.6 Hz, 2H, C_6H_4), 7.03 (d, *J* = 8.6 Hz, 2H, C_6H_4), 7.07 (d, *J* = 8.6 Hz, 2H, C_6H_4). ^{13}C NMR of *Z*+*E* Isomers ($CDCl_3$): δ (ppm): 20.7 and 21.3 (CH_3), 28.2 ($2CH_2$, succinimide), 29.3 (CH_2), 32.3 (CH_2), 38.8 (CH_2), 69.6 and 69.8 (2CH, C_5H_4), 70.0 (2CH, C_5H_4), 70.6 (5CH, Cp), 88.2 and 88.3 (C, C_5H_4), 115.4 (2CH, C_6H_4), 121.4 (2CH, C_6H_4), 130.6 (2CH, C_6H_4), 131.4 (2CH, C_6H_4), 134.8 (C), 136.5 (C), 138.1 (C), 141.9 (C), 149.1 (C), 154.6 (C), 169.4 and 169.6 (COO), 177.6 (2CO imide). IR (ATR, ν cm^{-1}): 3324 (OH), 1730 and 1750 (weak, CO), 1698 (strong, CO). HRMS (ESI, $C_{33}H_{31}FeNO_5$: $[M]^{+\cdot}$) calc: 577.1546, found: 577.1544.

Unambiguous differentiation of the *E* and *Z* isomers of **P998** and of **P849** by NMR spectroscopy was accomplished by use of the two-dimensional NOESY technique (see supplementary information and Figures S10 – S13)

Preparation of ferrocifen lipid nanocapsules (LNCs). LNCs were prepared using a phase inversion process as thoroughly described in litterature.[22] Briefly, the studied ferrocifen was added with Kolliphor® HS 15 (16.9 % *w/w*) and Labrafac® WL 1349 (20.7 % *w/w*) and stirred for 30 min at 60 °C. Then the other compounds (Lipoïd S 100 (1.5 % *w/w*), NaCl (1.3 % *w/w*, physiological osmolarity) and UPW (59.6 % *w/w*) were added and mixed under magnetic stirring at 60 °C for 10 min. Three heating-cooling cycles were performed between 90 °C and 60 °C to obtain a phase inversion of the emulsion (O/W emulsion for temperature lower than phase inversion temperature (PIT) and W/O emulsion for temperature higher than PIT). During the third cycle, when the temperature decreased and reached the PIT (78 °C < PIT < 83 °C), ice-cold UPW (31.5 % v/v_{tot}) was added to induce an irreversible shock to obtain the LNCs. Afterward, the suspension was stirred for 10 min under a slow magnetic stirring at room temperature. To finish, the LNC formulation was filtered through 0.2 µm sterile polyethersulfone (PES) membrane (Dutscher, Bernolsheim, France) to remove any unloaded ferrocifen before being stored at 4 °C. In order to show the benefit of filtration as a separation technique of free ferrocifen, a sedimentation step of unloaded ferrocifen from LNC formulation was performed. In practice, formulations were left to remain for 1h after the LNC formulation process before sample preparation for chromatographic analysis.

Characterization of LNCs. Average hydrodynamic diameter (Z-average) and polydispersity index (PDI) were determined by dynamic light scattering (DLS) at 25 °C with a backscatter angle of 173° using a Zetasizer Nano ZS system (Malvern Panalytical Ltd, Worcestershire, UK) after a dilution by 6650 of the formulations in UPW. The measured average values were calculated from the correlation functions fitted using an exponential fit (Cumulant approach), based on 3 runs, with more than 10 measurements for each run.
Zeta potentials of the nano-systems were measured using the laser Doppler micro-electrophoresis technique by a Zetasizer Nano ZS system (Malvern Panalytical Ltd, Worcestershire, UK). The measured average values were calculated from 3 runs with more than 10 measurements for each run, after a dilution by 100 of the formulations with UPW (pH = 8.3 at 25 °C). Smoluchowski's approximation was used to determine electrophoretic mobility for determination of the zeta potential. The measured average values were calculated from 3 runs, with more than 10 measurements for each run. For Z-average, PDI and zeta potential of P769-LNCs, measurements were performed before gel formation.
Nanoparticle Tracking Analysis (NTA) was performed to determine the nanoparticle concentration. NTA was carried out using the NanoSight NS300 (Malvern Instruments Ltd, UK) and the suspensions were diluted in ultrapure water in order to have optimum concentration to allow analysis of the software to track the movement of particle. Prior to each analysis, samples were filtered using a 0.20 µm Whatman™ Anotop™ filter. Ultrapure water and suspensions were infused in the sample chamber using a syringe pump at 80 µL/min rate. A 405 nm laser was used to illuminate the particles, and their Brownian motion was recorded into 60 s videos (25 fps) using the sCMOS type camera of the instrument. Subsequently, the NTA software (NTA 3.2 Dev Build 3.2.16) allowed for processing of the data. The nanoparticle concentration was obtained after correction by the dilution factor. The experiment was performed in triplicate.

Determination of encapsulation efficiency (E.E) and drug loading (D.L). Encapsulation efficiency and drug loading of the ferrocifens were determined using two Ultra-High-performance liquid chromatography (UPLC) methods. A C18 analytical column (ACQUITY UPLC® BEH C18 1.7 µm, 2.1 x 50 mm, Waters, Molsheim, France) was used at 20 °C. Quantification of the encapsulated ferrocifens was obtained by measurement of UV absorbance at λ = 450 nm, after a filtration step through a 0.2 µm pore size filter or by sedimentation to separate the encapsulated from the free ferrocifens. A dissolution step of LNCs was performed before analysis with the optimal solvent or mix of solvents for each ferrocifen. Analysis of the data was performed using Empower 3 software (Waters). For **P722** and the two isomers of **P849**, the C18 column was eluted at a flow rate to 0.2 $mL.min^{-1}$ with an isocratic method: acetonitrile/water (65/35 *v/v*). Calibration curves were established (at each analysis) by quantifying the area under the curves (AUCs) of [0.01 – 0.2] $mg.mL^{-1}$ ferrocifen solutions in blank LNCs dissolved by a 40-fold dilution in methanol/DMSO (90/10 *v/v*). The loaded LNCs were dissolved by a 40-fold dilution with methanol/DMSO (90/10 *v/v*) to have **P722** and **P849** concentrations in the appropriate concentration range, and quantification of ferrocifens was performed using the calibration curve. The injection volume was of 5 µL and the retention times were of 1.2 min, 1.9 min and 3.1 min for **P722**, **(*Z*)-P849** and **(*E*)-P849** respectively.
For analysis of **P769** and the two isomers of **P998**, the C18 column was eluted at a flow rate of 0.2 $mL.min^{-1}$ with a gradient of acetonitrile and water (Table 1). Calibration curves were established (at each analysis) by quantifying the area under the curves (AUCs) of [0.01 – 0.2] $mg.mL^{-1}$ ferrocifen solutions in blank LNCs dissolved by a 40-fold dilution in a mix of methanol/acetonitrile/DMSO (45/45/10 *v/v/v*). The loaded LNCs were dissolved by a 40-fold dilution with methanol/acetonitrile/DMSO (45/45/10 *v/v/v*) to have **P769** and **P998** concentrations in the appropriate concentration range, and quantification of the samples was performed using the calibration curve. The injection volume was of 5 µL and the retention times were of 3.4 min, 3.0 min and 2.8 min for **P769**,

(*Z*)-P998 and **(*E*)-P998**, respectively.
Encapsulation efficiency (E.E, %) of the corresponding ferrocifen into LNCs was calculated using the following equation:

$$E.E\ (\%) = \frac{(Initial\ ferrocifen\ conc.in\ LNCs - unencapsulated\ ferrocifen\ conc.in\ LNCs)}{Initial\ ferrocifen\ conc.\ in\ LNCs} \times 100$$

Drug loading of the corresponding ferrocifen into LNCs was calculated using the following equation:

$$D.L\ \left(\%\ \frac{w}{w}\right) = \frac{Mass\ of\ encapsulated\ ferrocifen\ in\ 1\ mL\ of\ LNC\ dispersion}{m(ferrocifen) + m(Labrafac®\ WR\ 1349\ ) + m(Kolliphor®\ HS\ 15\ ) + m(Lipoïd\ S\ 100)} \times 100$$

Table 1. Gradient elution for analysis of **P769**, **(*E*)-P998** and **(*Z*)-P998** with the UPLC system.

Time (min)	Flow rate (mL/min)	Phase A: Water/ACN (95/5 *v/v*) (%)	Phase B: ACN (%)
0	0.2	50	50
0.5	0.2	15	85
4	0.2	15	85
5	0.2	50	50
15	0.2	50	50

Rheological measurements. Viscoelastic properties of gels were measured using a Kinexus® rheometer (Malvern Panalytical Ltd, United Kingdom) with a cone plate geometry (diameter 40 mm, angle 2°) at 20 °C. Linear viscoelasticity domain was first determined by oscillatory strain sweeps at constant frequency of 1 Hz. In this regimen (strain amplitude fixed at 0.1 % for all analyses), the viscoelastic properties: elastic G' and viscous G'' moduli were measured by varying the oscillation frequency (from 0.1 to 10 Hz). Values of G' and G'' were taken at 1 Hz. All these experiments were performed at least three times.

Interfacial tension measurements. Measurements of interfacial tension were performed using a drop tensiometer device (Tracker Teclis, Longessaigne, France). Concretely, a 10 µL rinsing drop of triglyceride (Labrafac® WL 1349) was generated with an Exmire microsyringe (Probablo, Paris, France) in an optical glass container filled with a water phase. To keep the volume of the drop constant and so the surface area, piston movements of the syringe were controlled by a stepping motor. Interfacial tension, surface area and volume of the drop were obtained using Laplace equation after analysis of the drop profile recorded in real time (1 measurement each 10 s) for 6 h using a video camera connected to a computer. The triglyceride phase was concentrated with different ferrocifens in the range of [0.1 – 1.6] mg/g of triglyceride. All measurements were performed at least three times, at a temperature of 20.8 $\pm$ 0.3 °C. Values were taken at 6 h, when interfacial tension plateau was reached.

LNC degradation by esterase. A solution of esterase from porcine liver, at a molar ratio of 1:1 in **P769**, was added respectively to the suspensions of blank LNCs, **P722**-LNCs and **P769**-LNCs at 1.6 mg/mL (eq. 5.6 mg/g). Soon after, samples were put at 37 °C for 96 h. At different time intervals, samples were collected and analysed by DLS to follow the hydrodynamic diameter of LNCs. **P769** hydrolysis was also followed by liquid chromatography coupled to mass spectrometry (LC/MS) system (Waters 2695 Separations Module and micromass Quattro micro™, software Quattro micro, Waters, Molsheim France), with single ion recording (SIR) analysis. Method was developed on an Alliance® 2695 system (with a 150 x 2.0 mm, 5 µm Uptisphere C18 5ODB column (Interchim, France). Samples were eluted at 20 °C, at a flow rate of 0.2 mL.min^{-1} with a gradient of water + 0.1% formic acid/ACN + 0.1% formic

acid (Table 2). Detection was obtained by measurement of UV absorbance at λ = 450 nm. Retention time for **P769** was 8.6 min, for **(*Z*)-P998** was 7.8 min and **(*E*)-P998** was 7.4 min. Then, after the elution through the Uptisphere column, samples were analysed by MS using a SIR mode. **P769**, **(*Z*)-P998** and **(*E*)-P998** were detected at m/z 620, 578 and 578 respectively. All measurements were performed at least three times.

Table 2. Gradient elution of the LC-MS/MS method for **P769** hydrolysis

Time (min)	Flow rate (mL/min)	Phase A: Water + 0.1 % formic acid (%)	Phase B: ACN + 0.1 % formic acid (%)
0	0.2	50	50
0.5	0.2	15	85
4	0.2	15	85
5	0.2	50	50
15	0.2	50	50

Cell Culture. Ovarian cancer cell line SKOV3 was obtained from the American Type Culture Collection (ATCC) and maintained as recommended. The SKOV3 cell lines were grown in McCoy's 5A Medium, modified with sodium bicarbonate, without L-glutamine and supplemented with 10 % of Fetal Bovine Serum (FBS) and 1 % of penicillin/streptomycin. Cells were maintained in a humid atmosphere at 37 °C with 5 % CO_2. Cells were passaged once they were at about 70 % of confluence.

***In vitro* activity of free ferrocifens and ferrocifen LNCs.** 3-(4,5-Dimethylthiazol-2-yl)-5-(3-carboxymethoxyphenyl)-2-(-4-sulfo-phenyl)-2H-tetrazolium salt (MTS) assay was used to test the cytotoxicity of free ferrocifens and ferrocifen-LNCs (colorimetric assay based on the conversion of a tetrazolium salt into formazan). For *in vitro* mitochondrial activity, ferrocifen-LNCs at a concentration of 2 mM in ferrocifen were prepared. It corresponded to a concentration (mg/g of lipophilic excipient) of 3.74 mg/g, 3.63 mg/g, 4.33 mg/g and 4.03 mg/g for **P722**, **P849** (two isomers), **P769** and **P998** (two isomers) respectively.
Briefly, SKOV3 cells were seeded at 2.5 x 10^3 cells/well in 96-well plates containing 100 µL growth medium. After 24 h at 37 °C with 5 % CO_2, the medium was removed and cells were treated with the tested ferrocifens and ferrocifen LNCs at 2 mM diluted with McCoy's 5A Medium in order to test 8 concentrations. After 72 h of incubation, treatments were removed and 100 µL per well of a mix MTS + McCoy's 5A Medium was added for 2 h. Absorbance was measured at 490 nm using a spectrophotometric plate reader (SPECTRAmax M2, Molecular Devices, San Jose, USA). The Dose-Response curves were plotted with GraphPad Prism Software and the IC_{50} values were calculated using the polynomial curves. All experiments were performed at least three times.

Statistical analysis. Results obtained from the experiments were analyzed statistically using GraphPad Prism® software. Mean and standard deviation (SD) were determined, and values are represented as Mean ± SD. Significant differences between means, for all experiments, were analysed using a Kruskal-Wallis test followed by a Dunn's test for multiple comparisons. Differences were considered statistically significant for $p < 0.05$.

RESULTS AND DISCUSSION

Physico-chemical characterization of LNC formulations.

Encapsulation efficiency was obtained after separation of unloaded ferrocifen by filtration on 0.2 µm (Figure 2) or by sedimentation (Figure S1 in supplementary information), as its density is higher than the dispersive water phase. From these two techniques of separation, results obtained were in accord

with macroscopic observations made after LNC formulation: an orange precipitate was observed at the bottom of the vial corresponding to unloaded ferrocifen when the initial amount of ferrocifen was too high. The experimental results revealed that the encapsulation efficiency (E.E) of the diphenolic succinimido-ferrocifen **P722** in LNCs decreased with the initial amount added, from around 100 % of E.E with an initial amount below 7.0 mg/g of lipophilic excipients (**P722** + Labrafac® WL 1349 + Kolliphor® HS 15 + Lipoïd S100) (eq. 2 mg/mL of formulation) to values lower than 55 % with an initial amount above 13.9 mg/g (eq. 4 mg/mL of formulation). Maximal drug loading for **P722** was 7.0 mg/g of lipophilic excipients. It was a low amount compared to another potent ferrocifen, **P53** for which the maximal drug loading was 43.6 mg/g, and was recently explained by the higher lipophilicity of **P53** compared to **P722**.[25]

Thus, to improve the drug loading of the succinimido-ferrocifen family in LNCs, some minor structural modifications were carried out on **P722** leading to five new succinimido-ferrocifens that were expected to be more lipophilic: the monophenols **(*E*)** and **(*Z*)-P849**, the diester **P769**, and the monophenolic esters **(*E*)** and **(*Z*)-P998** (Figure 1). Gratifyingly, solubility experiments performed in caprylic/capric triglyceride (Labrafac® WL 1349) confirmed that these five molecules were more lipophilic than the diphenol **P722** (Table 3). Moreover, solubility values also explained the encapsulation behaviour of the different ferrocifens. Indeed, the monophenol **(*Z*)-P849** was found to be more lipophilic than its ***E*** counterpart, and had an E.E higher than 90%, whatever the initial amount added; in contrast, the E.E for **(*E*)-P849** decreased with the initial amount added, which might be explained by the difference in polarity between the two isomers. Likewise, the monophenolic ester **(*E*)-P998** had an E.E, higher than 90 % whatever the initial amount added, whereas **(*Z*)-P998** showed a decrease in its E.E until 60 % for an initial amount of 17.2 mg/g (eq. 5 mg/mL). However, due to facile *E*/*Z* isomerization, each initially chromatographically pure sample of **P998** eventually contains a minor fraction of the other isomer: **(*E*)-P998** evolved to the ratio *E*/*Z* ≈ 74/26, whereas for **(*Z*)-P998**) *Z*/*E* ≈ 87/13. **(*E*)-P849** and **(*Z*)-P849** isomerize more slowly to yield the ratio ≈ 92/8. Finally, the E.E obtained from the diester **P769** was higher than 90 %, but it was not possible to determine an E.E above an initial amount of 8.7 mg/g because of gel formation (Figure 2 and Figure S1 in supplementary information).

All hydrodynamic diameters were around 50 nm whatever the initial amount of ferrocifen added, and all the PDI measured were below the limiting value of 0.2, allowing one to consider each of the ferrocifen-LNCs as a monodisperse suspension (Figure 3). Moreover, whatever the ferrocifen encapsulated, zeta potentials of LNCs were not impacted with values below - 5 mV, close to neutrality (Figure S2 in supplementary information). Results obtained were in accordance with previous studies performed in the MINT laboratory.[21,27,28]

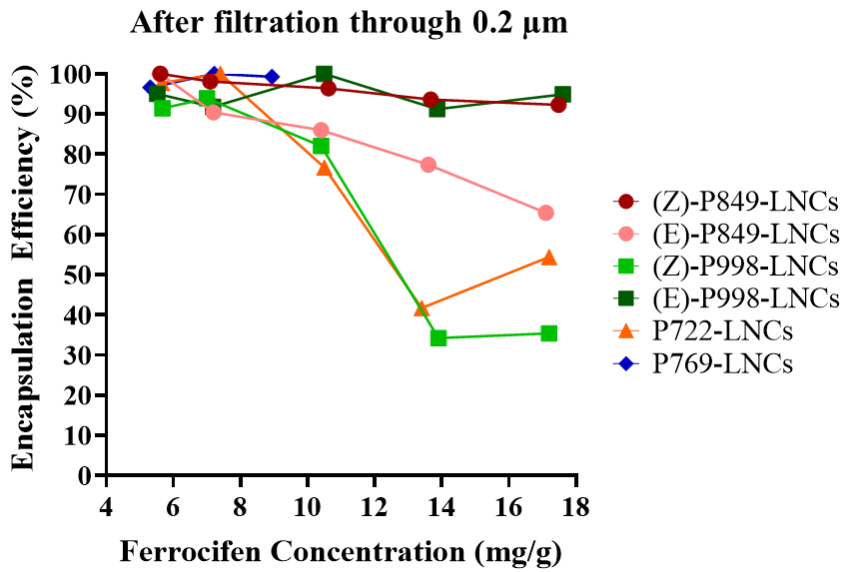

Figure 2: Encapsulation efficiency (E.E) (%) of succinimido-ferrocifen molecules in LNCs according to initial amounts of ferrocifens after filtration through 0.2 µm pore size filter. Ferrocifen concentration is expressed according to the weight of all lipophilic excipients (ferrocifen + Labrafac® WL 1349 + Kolliphor® HS 15 + Lipoïd S100) (n = 1).

Table 3: Solubility in caprylic/capric triglycerides (Labrafac® WL 1349) of the different succinimide-ferrocifens (n = 1).

Ferrocifen	Solubility in Labrafac® WL 1349 (mg/g)
P722	0.12
(Z)-P849	5.45
(E)-P849	2.11
P769	4.04
(Z)-P998	0.87
(E)-P998	2.64

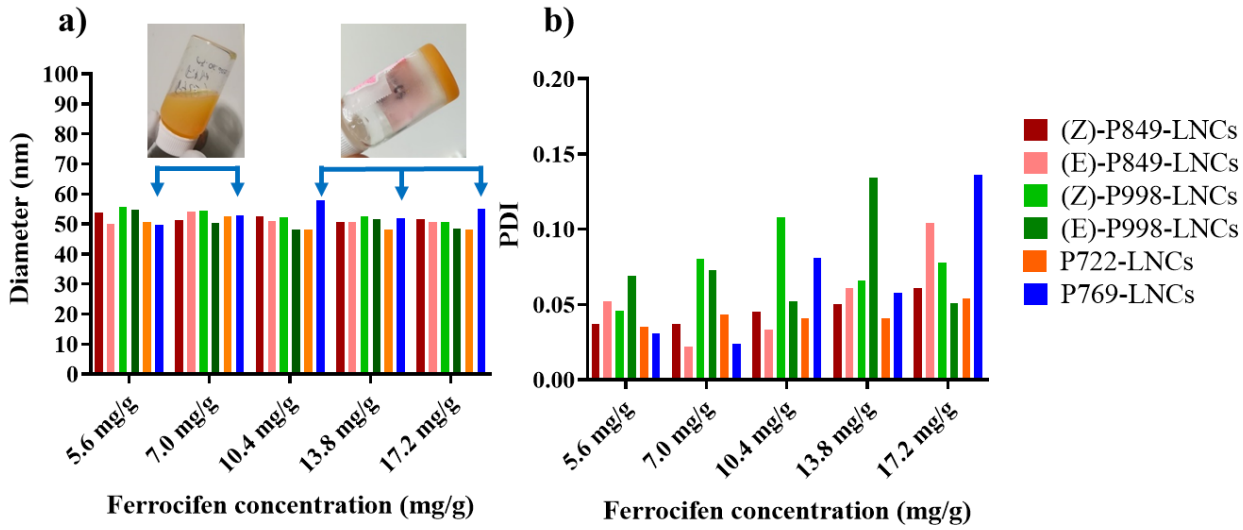

Figure 3: Physico-chemical characteristics of ferrocifen lipid nanocapsules (LNCs) obtained by Dynamic Light Scattering (DLS): a) Hydrodynamic diameter of ferrocifen-LNCs. A gel was obtained for diester **P769** at 10.4 mg/g, 13.8 mg/g and 17.2 mg/g as shown on the photo; b) Polydispersity index (PDI) of ferrocifen-LNCs. Values for P769-LNCs, from 10.4 mg/g to 17.2 mg/g, were obtained before the formation of the gel. Results are repetitions of three measurements for each sample (n = 1).

Rheological characterisation of acetyl-ferrocifen-LNC gel.

As explained previously, a gel was obtained with the diester **P769** for a payload higher than 8.7 mg/g (Figure 2 and Figure S1 in supplementary information). Measurement of the viscoelastic properties of **P769**-LNC gel, from 10.4 mg/g to 17.2 mg/g, were performed after gel formation (one night at 4 °C). First, the linear viscoelasticity region was determined by strain amplitude sweep at constant oscillation frequency of 1 Hz. A linear regime, corresponding to strain-independent elastic moduli (G') and viscous moduli (G"), was identified (Figure S3 in supplementary information). Then, the viscoelastic properties were measured with frequency sweep from 0.1 to 10 Hz at a fixed strain amplitude of 0.1 % (Figure S3 in supplementary information). For each measurement, G' and G" values were constant and G' was higher than G" (Table S1 in supplementary information). These preliminary results confirmed that this system obtained after encapsulation of **P769** in LNCs (for concentration higher than 10.4 mg/g) can be phenomenologically defined as a gel.[29]

The influence of **P769** concentration and LNC concentration (number of particles per mL of formulation) on the rheological behaviour of the gel was then studied. First, G' and G" values increased significantly from 17.9 ± 4.4 to 144.4 ± 8.1 Pa for G' and 2.9 ± 1.3 to 28.3 ± 4.4 Pa for G" when the **P769** concentration increased from 10.4 to 17.2 mg/g, respectively (Figure 4.a). Even if gel hardness seemed to be lost with the decrease in **P769** concentration (from macroscopic observations), **P769**-LNCs gel elasticity (defined by G'/G'' ratio) was not significantly changed whatever the **P769** concentration: 7.9 ± 4.5, 4.9 ± 1.7 and 5.4 ± 1.2 for **P769** payload of 10.4 mg/g, 13.8 mg/g and 17.2 mg/g, respectively (Table S1 in supplementary information). The same rheological behaviour was obtained with variation of LNC concentration, for a constant **P769** concentration of 17.2 mg/g. Indeed, when decreasing the concentration in nanoparticles (from 2.72×10^{15} to 6.6×10^{14} LNC/mL), G' and G'' values significantly decreased, from 144.43 ± 8.1 to 13.68 Pa for G' and from 28.3 ± 4.4 to 2.9 ± 1.3 Pa for G'' (Figure 4.b). As for the results obtained with variation of **P769** concentration, elasticity of the gel was unchanged whatever the LNC concentration (Table S1 in supplementary information).

To conclude this section, **P769** concentration and LNC concentration are the two important parameters towards obtaining a **P769**-LNC gel. However, this is not the first time that a gel made of LNCs has been obtained. Indeed, in 2013 Moysan et *al.* reported a gel made of LNCs loaded with an amphiphilic gemcitabine, modified by a lipid tail. They showed that its rheological behaviour was dependent on LNC concentration, and also on modified-gemcitabine concentration with a constant elasticity.[30] Moreover, an article published in 2021 also showed the same characteristics of a gel made of LNCs and an amphiphilic cytidine.[31] In that case, gel formation was rationalized in terms of hydrogen bonding between cytidine heads localized at the LNC surface.

In our study, **P769** was prepared with the idea of esterification of the two phenol functions to increase the **P722** lipophilicity. This modification allowed the formation of **P769**-LNC gel. To the best of our knowledge, this is the first time that such a structure has been obtained with a ferrocifen. All studies previously performed on ferrocifen-LNCs showed only the formation of a suspension, compatible with an intravenous administration route, with promising results on several cancers.[23,26,32,33] For the **P769**-LNC gel, use as local therapy to treat glioblastoma after tumour resection could be imagined, as ferrocifens have already shown efficacy against this cancer.[34–36] Indeed, Vessières *et al.* showed a large heterogeneity of response to **P722** on Patient-Derived-Cell-Line glioblastoma depending on transcriptomic subtypes.[37] A more recent study also highlighted the efficiency of **P722** complexed with cyclodextrins on glioblastomas.[24] Moreover, **P769** was tested on the U87MG glioblastoma cell line, with or without LNCs, and the IC_{50} values obtained were 67 nM and 46 nM, respectively, close to the 27 nM obtained with **P722** alone, after 96 h of treatment.[38] Taking all these results together, it could open new opportunities for the personalized treatment of glioblastomas.

Then, to check injectability of **P769**-LNC gel, at 17.2 mg/g, rheological measurements were performed after extrusion through 18 G and 26 G needles. Results obtained were compared to the control, without extrusion (Figure 4.c). After extrusion through a 26 G needle, significant differences were obtained on G' and G'' values. Indeed, a decrease was obtained, from 144.4 ± 8.1 to 50.0 ± 15.3 Pa for G' and from 28.3 ± 4.4 to 14.2 ± 4.0 Pa for G'', without or after extrusion, respectively. However, elasticity remained constant (Table S1 in supplementary information). After an extrusion through 18 G needle, no significant difference was observed even if a small decrease was obtained from 144.4 ± 8.1 to 90.1 ± 6.5 Pa for G' and from 28.3 ± 4.4 to 18.4 ± 1.4 Pa for G'', without or after extrusion, respectively. As after extrusion through a 26 G needle, elasticity remained constant (Table S1 in supplementary information). These results confirmed the injectability of **P769**-gel. The same results were obtained after an extrusion through 18 G needle for modified gemcitabine-LNCs and modified cytidine-LNC hydrogels.[30,31]

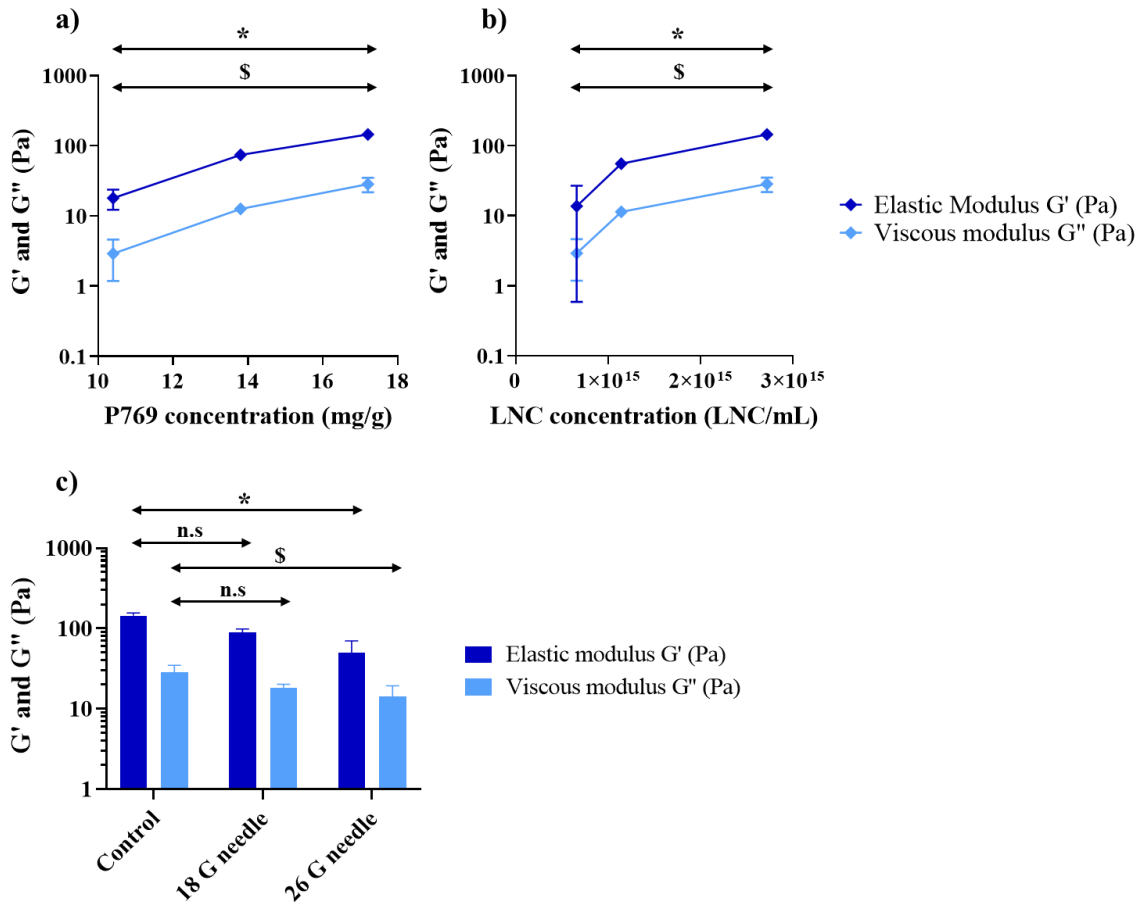

Figure 4: a) Elastic G' (dark blue) and viscous G'' (light blue) moduli according to **P769** concentration, with 2.72 x 10^{15} LNC/mL ; b) Elastic G' (dark blue) and viscous moduli G'' (light blue) according to nanoparticle concentration, at a **P769** concentration of 17.2 mg/g. c) Elastic G' and viscous G'' moduli after extrusion through 18 G and 26 G needles of **P769**-LNC gel at 17.2 mg/g. G' and G'' values are taken at a strain amplitude of 0.1 % and a frequency of 1 Hz at T = 20 °C (n = 3, mean ± SD, *: $p < 0.05$ for elastic modulus, $: $p < 0.05$ for viscous modulus).

While studying the monophenolic ester succinimido-ferrocifen **P998** (both isomers), an unexpected and interesting phenomenon was observed whereby a gel made from **(*E*)-P998**-LNCs was obtained above a limiting concentration, whereas no gelification process was observed with **(*Z*)-P998**-LNCs, whatever the ferrocifen concentration. Rheological measurements revealed the influence of **(*E*)-P998** concentration on the viscoelastic properties. Indeed, G' and G'' values increased significantly from 14.4 ± 14.1 to 542.0 ± 103.5 for G' and 1.9 ± 1.7 to 108.8 ± 28.6 for G'' when the **(*E*)-P998** concentration increased from 17.2 mg/g to 33.9 mg/g, respectively (Figure 5). Moreover, above 17.2 mg/g, whatever the **(*E*)-P998** concentration, elasticity remained constant, as for the diester **P769** (Table S1 in supplementary information).

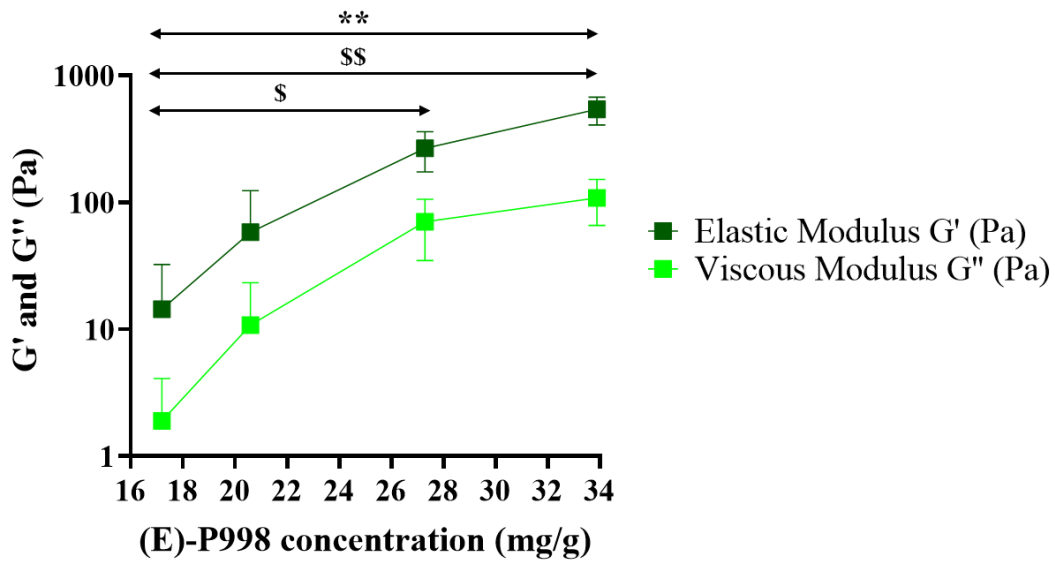

Figure 5: Elastic G' (dark green) and viscous G'' (light green) moduli according to the **(*E*)-P998** concentration. G' and G'' values are taken at a strain amplitude of 0.1 % and a frequency of 1 Hz at T = 20 °C ($3 < n < 5$, mean ± SD; *: $p < 0.05$, **: $p < 0.01$ for elastic modulus, $: $p < 0.05$, $$: $p < 0.01$ for viscous modulus).

The measured complex viscosity according to the oscillation frequency for **(*Z*)-P998**-LNCs, **(*E*)-P998**-LNCs and **P769**-LNCs confirmed the macroscopic observations. At a same concentration, 17.2 mg/g, **(*Z*)-P998**-LNCs showed constant viscous behaviour whatever the oscillation frequency, whereas a linear decrease of the viscosity was obtained for **(*E*)-P998**-LNCs (Figure 6), characteristic of the shear thinning flow behaviour of gels. A higher concentration in monophenolic ester **(*E*)-P998** was needed to obtain a gel with similar viscoelastic properties compared to the diester **P769** (Figures 5 and 6) an observation possibly explicable in terms of the facile isomerisation of **P998** leading to a mixture of **(*E*)** and **(*Z*)-P998**.

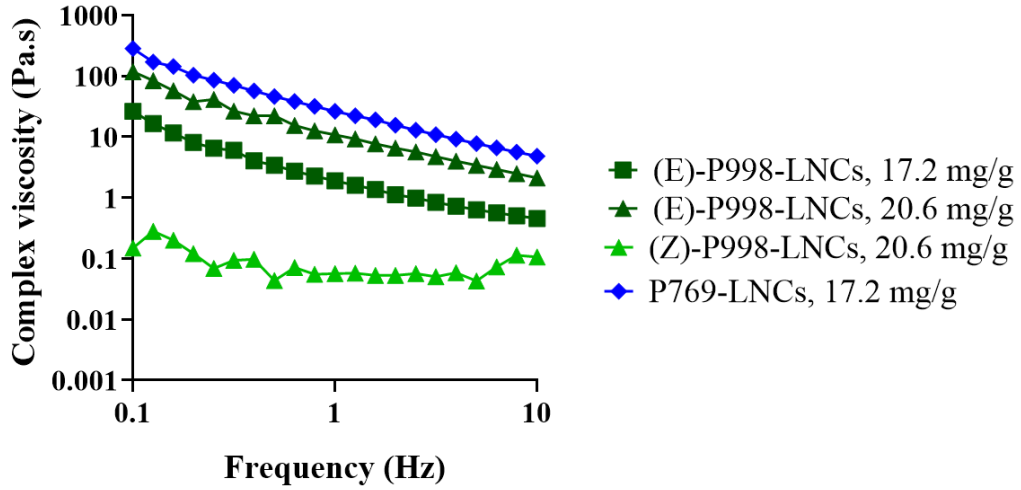

Figure 6: Complex viscosity according to the oscillation frequency for: **P769** loaded LNCs, 17.2 mg/g (dark blue diamond), **(*E*)-P998** loaded LNCs, 17.2 mg/g (dark green square), **(*E*)-P998** loaded LNCs, 20.6 mg/g (dark green triangle) and **(*Z*)-P998** loaded LNCs, 20.6 mg/g (light green triangle). Strain amplitude of 0.1 %, at T = 20 °C ($3 < n < 5$, mean ± SD).

These results highlighted the importance of the acetylation position on the succinimido-ferrocifen structure. Having the acetyloxyphenyl ester group positioned *cis* to the propylsuccinimido moiety, i.e. *trans* to the ferrocenyl moiety, appears to be an essential condition to obtain a gel structure. We note, however, that esterification of the phenol ring in ferrocifens was reported in earlier work by Allard *et al.* in 2009, whereby formulations of LNCs loaded with acetylated-ferrocifenols (entitled Fc-diAc), but lacking the succinimido moiety, were prepared with the aim of treating glioblastomas. Whatever the concentration used, no gel was obtained with these ferrocifens.[39] Moreover, formulations of **P996**-LNC, in which a third acetyl unit, rather than an imido moiety, was incorporated at the terminus of the propyl chain, did not yield a gel at concentrations of 17.2 mg/g and 34.4 mg/g (Figure S4 in supplementary information).[40] These results seem to confirm the importance for gel formation of having a succinimido moiety positioned *cis* to the acetylated phenolic group.

Position in the LNCs depending on the molecular structure.

To better understand gel formation, interfacial tension measurements were performed using drop tensiometry to determine the ferrocifen position in LNCs. Surface tension, at the molecular level, results from the difference in energy between molecules at a fluid interface and in the bulk.[41] We here offer the following hypothesis: the diester **P769** should be sited at the surface of LNCs and so act as a surfactant, whereas diphenol **P722** and the corresponding monophenolic ester succinimido-ferrocifen **P849** will be encapsulated within the core of the LNCs. First of all, interfacial tension of a pendant drop mimicking blank LNCs, **P722**-LNCs and **P769**-LNCs suspensions at the air/water interface was measured (see supplementary information). The surfactant properties of blank LNCs have already been described in the literature, leading to a decrease of the surface tension at the air/water interface.[42] However, the results obtained in this study did not reveal any difference in interfacial tension, whatever the suspension used (Figure S5 in supplementary information). This may be explained by the low ferrocifen content compared to that of the hydroxystearate polyethylene glycol, the main surfactant in LNCs. Hence, a simplified model was used to test the hypothesis. A triglyceride (Labrafac® WL 1349)-water interface study was performed by measuring interfacial tension of a rising triglyceride drop, with or without ferrocifen, in a bulk water phase. Because of its low solubility in triglyceride, no measurement with diphenol **P722** could be performed.

The diester **P769** showed amphiphilic properties (Figure 7.a) whereby the interfacial tension significantly decreased with concentration, from 22.83 ± 1.21 to 16.45 ± 0.35 mN/m at 0 mg/g and 1.6 mg/g respectively. The same experiments were carried out with the modified-gemcitabine and the modified-cytidine.[30,31] During the adsorption kinetics, **P769** moved from the Labrafac drop to the Labrafac/water interface and acted as a surfactant. Such behaviour was not observed for the monophenol **P849** whereby, at the same concentration of 1.0 mg/g, the interfacial tension did not decrease (Figure 7.b). For the monophenolic ester **P998**, it was more difficult to interpret the results, perhaps because of the fast isomerisation of **P998** leading to a mixture of ***E*** and ***Z*** isomers, both of which led to a small decrease of the interfacial tension, from 22.83 ± 1.21 to 21.28 ± 0.39 and 20.23 ± 0.68 mN/m respectively.

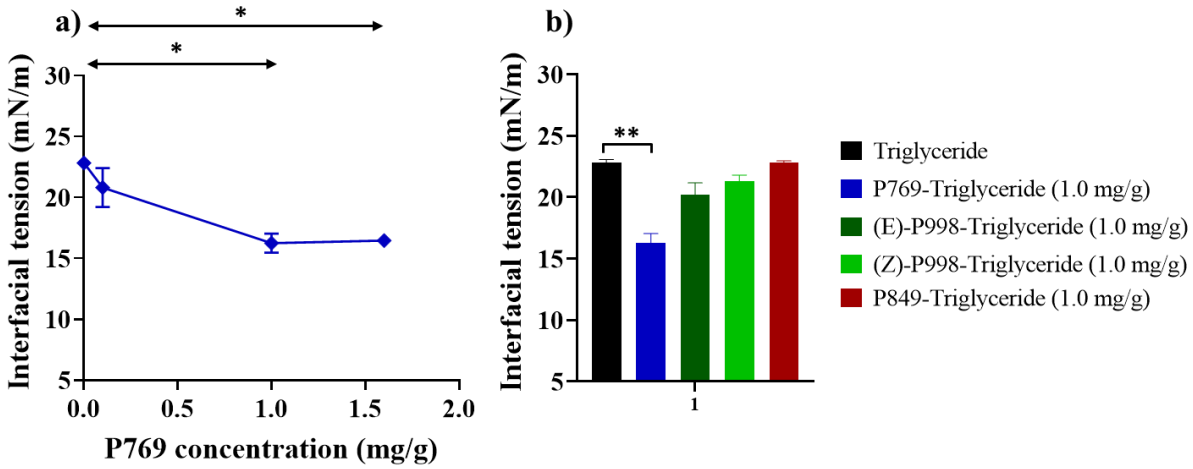

Figure 7: a) Interfacial tension measurements of a 10 µL triglycerides (Labrafac) drop in contact with a water phase according to diester **P769** concentration in the oil drop; b) Interfacial tension of a 10 µL triglyceride drop in contact with a water phase according to the ferrocifen used, at 1.0 mg/g of triglycerides in ferrocifens ($3 < n < 4$, mean ± SD; *: $p < 0.05$, **: $p < 0.01$). Values were taken at 6 h, when interfacial tension plateau was reached.

To confirm the results of the interfacial tension measurements, a kinetics study of LNC destabilisation was performed in the presence of esterase at 37 °C. LNCs exhibit a core-shell structure composed of a liquid triglyceride core and an amorphous polyethylene glycol hydroxystearate surfactant shell.[22] An esterase should catalyse the hydrolysis of esterified PEGylated surfactant of LNCs, as shown in the literature for PEGylated vesicles and PEGylated solid lipid nanoparticles.[43,44] This "dePEGylation" could result in LNC membrane destabilisation, and so an increase of the LNC diameter. Moreover, from the interfacial measurement, **P769** seems to be at the LNC surface, and its acetate functional group could be predisposed to be hydrolysed by esterase (Figure S6 in supplementary information). Thus, the possible competitive cleavage of the **P769** acetate group or of the PEG was followed by DLS and by LC/MS (SIR analysis) (Figure 8**)**. Whatever the formulation, as expected, the LNC hydrodynamic diameter was not modified after an incubation with water for 96 h at 37 °C. However, it was possible to see differences in the presence of esterase. Indeed, a significant difference was obtained on the **P769**-LNC and the **P722**-LNC diameters with increases of 7.8 ± 1.7 and 24.6 ± 3.8 %, respectively, after 24 h of incubation. After 96 h of incubation, the same tendency was observed between **P722**-LNCs and blank LNCs. A significant difference was also obtained between **P769**-LNCs and **P722**-LNCs with an increase in LNC diameter of 11.9 ± 1.0 % and 39.2 ± 4.7, respectively (Figure 8.a). This difference of behaviour with esterase may be associated with the competitive hydrolysis of **P769** and of polyethylene glycol hydroxystearate at the surface of the LNCs, as explained. Moreover, by mass spectrometry, a stability study was performed on **P769**-LNC and the two isomers of **P998** that were obtained after 24 h of incubation with esterase, with retention times of 8.63 min, 7.83 min and 7.39 min for **P769**, **(*Z*)-P998** and **(*E*)-P998**, respectively (Figure 8.b).

To study the possible molecular interactions responsible for the gel formation, ethanol, urea and NaCl were added to determine possible van der Waals, hydrogen-bonding, or electrostatic interactions, respectively (Method description and Figure S7 in supplementary information): no difference in terms of rheological properties was observed on **P769**-LNC gel, thus implying that hydrogen bonding is not the controlling phenomenon. Hence, from all these results, the following hypothesis was advanced: the diester **P769** should be sited at the LNC surface and a possible interaction as the origin of the

development of the network could arise from interaction between a lone pair of a carbonyl group of the succinimido moiety with the plane of the neighbouring arene ring as shown schematically in Figure 9. The LP-π interaction is now more commonly invoked[45] and has already been shown to confer additional stability on the corresponding quinone methide of **P722**.[17] However, this phenomenon should not be observed with the diphenol **P722** as it would be localized in the oily core of LNCs. Such an approach accounts not only for the behaviour of the diester **P769**, but also for the specific case of the *E* isomer of the monophenolic ester **P998**. While the detailed mechanism of the LP-π interaction has been the source of some controversy, the presence of the electron-withdrawing ester group, rather than a simple phenol, should help to polarize the arene ring thereby enhancing the interaction. We note that in the solid state the diphenol **P722** adopts a conformation such that the succinimido and aryl rings are almost parallel, and it is only in the corresponding quinone methide that the LP-π interaction is found, as evidenced by its X-ray crystal structure in which they are positioned almost orthogonal to each other. Furthermore, one can readily visually a doubling of this interaction as depicted in Figure 9.

Even though some ferrocifens have already been assumed to be at the LNC surface,[26] this is the first occasion on which a gel is observed. Indeed, for the ferrocifen **P15** (or Fc-OHTam), the zeta potential, representing the surface charge of the LNCs, became positive: it remained negative with the other ferrocifens (Figure S2 in supplementary information). This increase of zeta potential was probably due to the positively charged dimethylamino moiety *cis* to the ferrocene moiety in **P15**.[26]

As for the modified gemcitabine-LNC gel, this **P769**-LNC gel is different in nature from the conventional ones. Indeed, in the literature, most nanoparticle-loaded hydrogels are obtained with the use of a natural or synthetic polymer matrix.[46] In this study, the **P769**-LNC gel obtained is polymer-free, made up only of the drug loaded nanoparticles, limiting potential side effects from the polymer, and improving the global drug loading of the system.

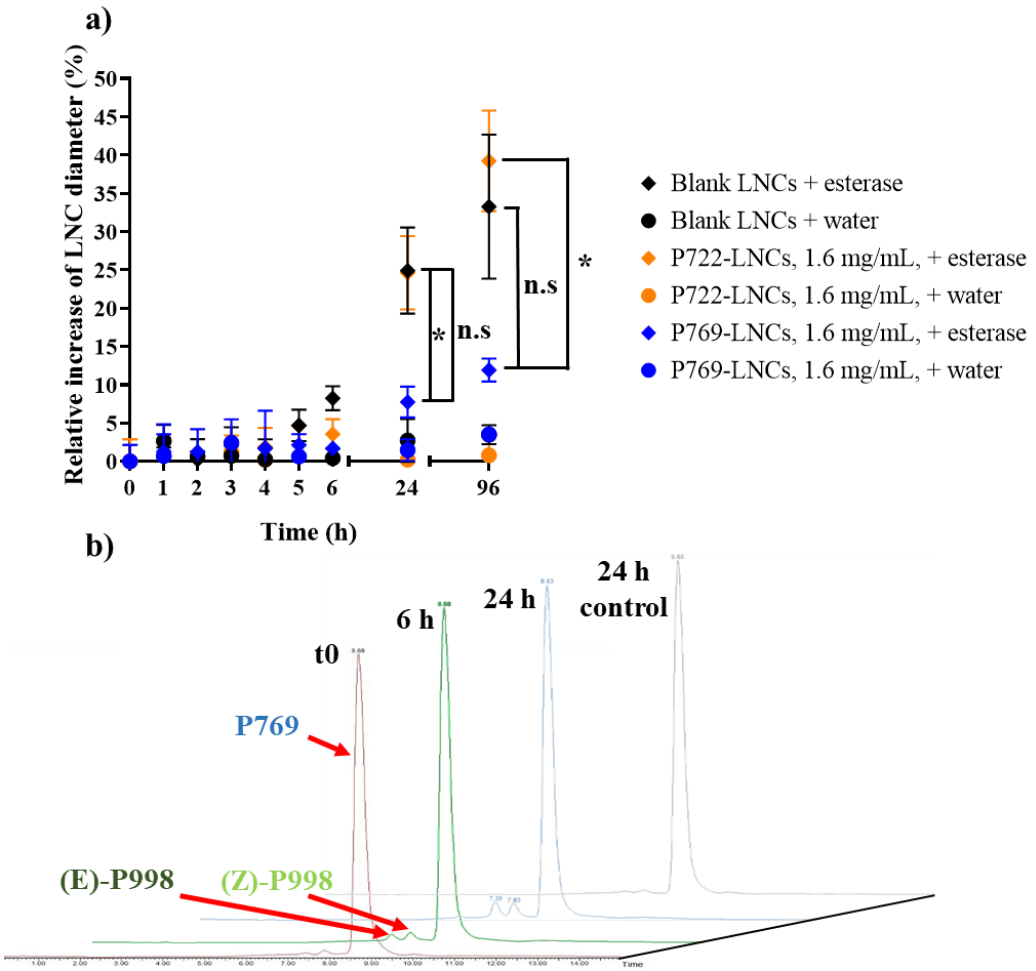

Figure 8: a) Relative increase of LNC diameter in the presence of water (circle) or in the presence of esterase (diamond) for blank LNCs (black), **P769**-LNCs, 1.6 mg/mL (dark blue) and **P722**-LNCs, 1.6 mg/mL (orange) ($3 < n < 5$), mean ± SD; *: $p < 0.05$).; b) Chromatograms (LC-MS) showing the kinetics of deacetylation of **P769**: t0 (red), t = 6 h (green), t = 24 h (blue) and t = 24 h (dark) for control. **P769** deacetylation led to the mono-acetyl **P998**. The chromatograms have been shifted for better clarity.

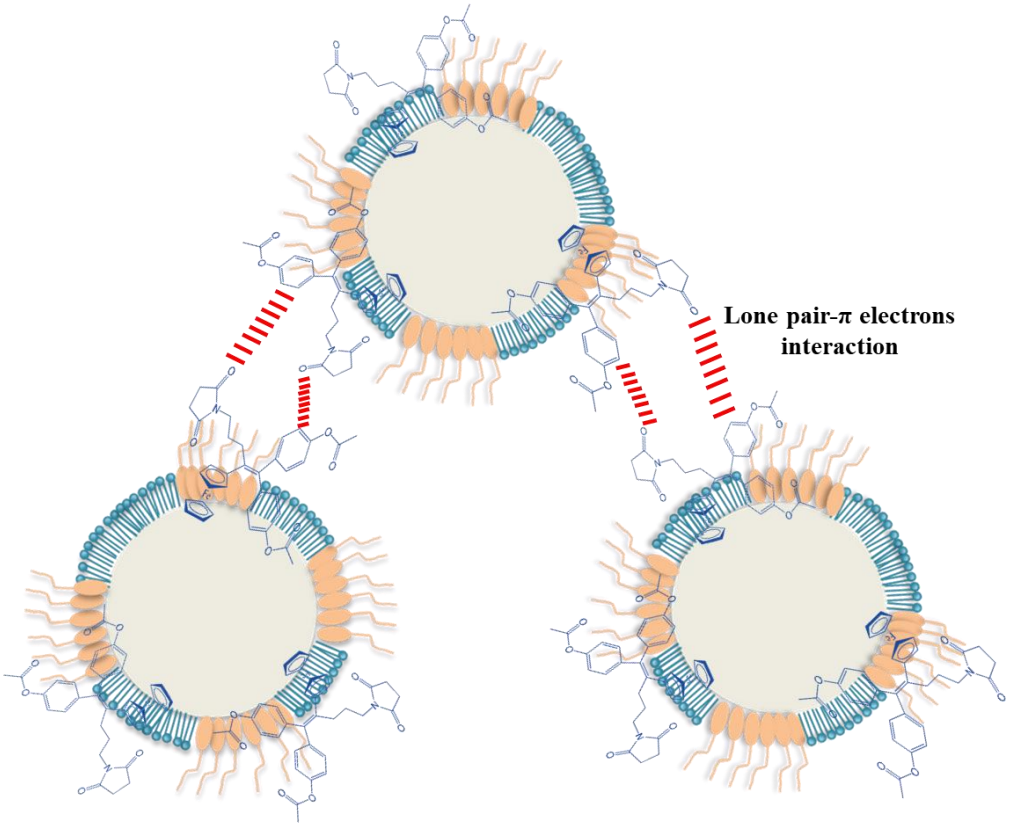

Figure 9: Graphical representation of the possible interaction at the origin of **P769**-LNC gel network. The red dotted line represents the lone pair-π interaction.

***In vitro* activity of ferrocifen-LNCs on ovarian SKOV3 cell line.**

In vitro activity of free ferrocifens and ferrocifen-LNCs suspensions was studied on the ovarian tumour cell line SKOV3 after 72 h of treatment (Figure 10, and Figure S8 in supplementary information). For all the ferrocifen-LNC suspensions, the IC_{50} values obtained were in the range of [0.1 – 0.6] µM, attributable to the presence of the ferrocifen. Indeed, blank LNCs did not show any cytotoxicity effect at the same dilution as for ferrocifen-LNCs (Figure 10). Moreover, no difference in IC_{50} was observed when the different ferrocifens were free or encapsulated in LNCs, confirming results from the literature that LNCs did not alter the ferrocifen efficacy.[21,23,47] Moreover, it was possible to distinguish two slopes on cell viability depending on ferrocifen concentration. This could be associated with a senescence mechanism at low concentrations, as already described for **P722**,[24] and also for the ansa-ferrocifen **DP1**,[48] followed by an apoptotic mechanism at higher concentrations.[24] Finally, chemical modification performed on the initial **P722** did not significantly hamper its efficiency. For the monophenol-succinimido-ferrocifen, **(*Z*)-P849**, similar biological activity has already been observed on the MDA-MB-231 breast cancer cell line.[17] Moreover, previous studies performed with another diacetylated ferrocifen, Fc-diAc, showed that its activity was the same as for the diphenol Fc-diOH, suggesting that esterase found in living cells led to a fast hydrolysis of the acetate groups.[39,49] Thus, the same scenario will certainly be followed with diester **P769**, or **(*E*)** and **(*Z*)-P998**, to recover the initial **P722**, whatever its position in the LNCs.

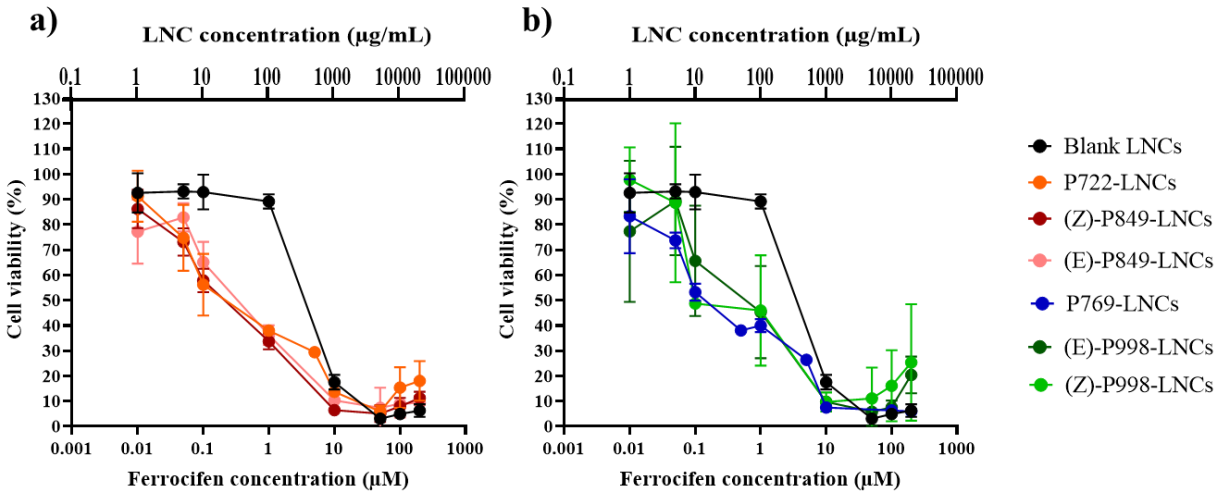

Figure 10: Cell viability of SKOV3 cells after 72 h of treatment with several concentrations of: a) Blank LNCs (black circle), **P722**-LNCs (orange circle), **(*Z*)-P849**-LNCs (dark red circle) and **(*E*)-P849**-LNCs (pink circle); b) Blank LNCs (black circle), **P769**-LNCs (dark blue circle), **(*E*)-P998**-LNCs (dark green circle) and **(*Z*)-P998**-LNCs (green circle). For each ferrocifen, at equal concentration, same dilution of LNCs was done (n = 3, mean ± SD).

CONCLUSION

In this study, one of the most promising ferrocifens, the diphenol **P722** in the succinimide-ferrocifen family, was first encapsulated in LNCs. Because of its weak drug loading, minor chemical structural modifications were performed to increase the lipophilicity of **P722**. These modifications led to an increase in the maximal drug loading in LNCs by a factor of three for some ferrocifens (**(*E*)-P998** and **(*Z*)-P849**). Interestingly, the other isomers **(*Z*)-P998** and **(*E*)-P849** did not show the same tendency with a decrease of the encapsulation efficiency when the drug concentration increased. Another unexpected result was the formation of a gel with two ferrocifens, the diester succimido-ferrocifen **P769** at concentration higher than 10.4 mg/g, and the monophenolic ester succinimido-ferrocifen **(*E*)-P998** at concentrations higher than 17.2 mg/g. The rheological measurements highlighted the injectability of the **P769**-LNC gel using a syringe and the importance of the motif [*cis*-propylsuccinimido-ene-phenyl-acetate] on the drug delivery system obtained. This gel formation was rationalised in terms of the spatial disposition of **P769** at the LNC surface, coupled with intermolecular lone pair- π interactions, as shown by interfacial measurements. To the best of our knowledge, it is the first time that a structure-drug delivery system relationship has been demonstrated for ferrocifens. Knowing that ovarian cancer metastases mostly in the peritoneal cavity, together with the remarkable *in vivo* efficacy on several cancers of **P722** (glioblastoma[24], metastatic melanoma[23], ovarian cancer[25]), we can see new opportunities for the use of **P769**-LNCs gels as local therapies to combat glioblastomas or peritoneal metastatic ovarian cancers.

AUTHOR INFORMATION

Corresponding author

* Elise Lepeltier: elise.lepeltier@univ-angers.fr

Author contributions

All authors have contributed to the manuscript and have given approval to the final version.

ACKNOWLEDGMENTS

The authors would like to thank the SME Feroscan for its supply of ferrocifens and the COST Action STRATAGEM, CA17104. This work was funded by the Agence Nationale de la Recherche (ANR PRCE NaTeMOc N° ANR-19-CE18-0022-01).

CONFLICT OF INTEREST

The authors declare no conflict of interest. The authors declare no competing financial interest or personal relationships that could have appeared to influence the work reported in this paper.

SUPPORTING INFORMATION

Supplementary information about experimental; encapsulation efficiency of ferrocifens after sedimentation; zeta potential values of ferrocifen loaded LNCs; rheological properties; interfacial tension measurements; determination of interactions responsible to gelification; cell viability; NMR spectra and IR spectrum of ferrocifens.

REFERENCES

(1) Couvreur, P. Nanomedicine: From Where Are We Coming and Where Are We Going? *J Control Release* **2019**, *311–312*, 319–321. https://doi.org/10.1016/j.jconrel.2019.10.020.

(2) Uziely, B.; Jeffers, S.; Isacson, R.; Kutsch, K.; Wei-Tsao, D.; Yehoshua, Z.; Libson, E.; Muggia, F. M.; Gabizon, A. Liposomal Doxorubicin: Antitumor Activity and Unique Toxicities during Two Complementary Phase I Studies. *J. Clin. Oncol.* **1995**, *13* (7), 1777–1785. https://doi.org/10.1200/JCO.1995.13.7.1777.

(3) Zhao, M.-D.; Li, J.-Q.; Chen, F.-Y.; Dong, W.; Wen, L.-J.; Fei, W.-D.; Zhang, X.; Yang, P.-L.; Zhang, X.-M.; Zheng, C.-H. Co-Delivery of Curcumin and Paclitaxel by "Core-Shell" Targeting Amphiphilic Copolymer to Reverse Resistance in the Treatment of Ovarian Cancer. *Int J Nanomedicine* **2019**, *14*, 9453–9467. https://doi.org/10.2147/IJN.S224579.

(4) Huang, S.; Liu, H.; Huang, S.; Fu, T.; Xue, W.; Guo, R. Dextran Methacrylate Hydrogel Microneedles Loaded with Doxorubicin and Trametinib for Continuous Transdermal Administration of Melanoma. *Carbohydr Polym* **2020**, *246*, 116650. https://doi.org/10.1016/j.carbpol.2020.116650.

(5) Sun, H.; Chen, C.-K.; Cui, H.; Cheng, C. Crosslinked Polymer Nanocapsules. *Polymer International* **2016**, *65* (4), 351–361. https://doi.org/10.1002/pi.5077.

(6) Sun, H.; Erdman III, W.; Yuan, Y.; Mohamed, M. A.; Xie, R.; Wang, Y.; Gong, S.; Cheng, C. Crosslinked Polymer Nanocapsules for Therapeutic, Diagnostic, and Theranostic Applications. *WIREs Nanomedicine and Nanobiotechnology* **2020**, *12* (6), e1653. https://doi.org/10.1002/wnan.1653.

(7) Yang, C.; Lin, Z.-I.; Chen, J.-A.; Xu, Z.; Gu, J.; Law, W.-C.; Yang, J. H. C.; Chen, C.-K. Organic/Inorganic Self-Assembled Hybrid Nano-Architectures for Cancer Therapy Applications. *Macromolecular Bioscience* **2022**, *22* (2), 2100349. https://doi.org/10.1002/mabi.202100349.

(8) Coppens, E.; Desmaële, D.; Naret, T.; Garcia-Argote, S.; Feuillastre, S.; Pieters, G.; Cailleau, C.; Paul, J.-L.; Prost, B.; Solgadi, A.; Michel, J.-P.; Noiray, M.; Couvreur, P.; Mura, S. Gemcitabine Lipid Prodrug Nanoparticles: Switching the Lipid Moiety and Changing the Fate in the Bloodstream.

Int J Pharm **2021**, *609*, 121076. https://doi.org/10.1016/j.ijpharm.2021.121076.

(9) Jaouen, G.; Vessieres, A. Transition Metal Carbonyl Oestrogen Receptor Assay. *Pure Appl. Chem.* **1985**, *57* (12), 1865–1874. https://doi.org/10.1351/pac198557121865.

(10) Jaouen, G.; Vessieres, A.; Top, S.; Ismail, A. A.; Butler, I. S. Metal Carbonyl Fragments as a New Class of Markers in Molecular Biology. *J. Am. Chem. Soc.* **1985**, *107* (16), 4778–4780. https://doi.org/10.1021/ja00302a030.

(11) Jaouen, G.; Vessières, A.; Top, S. Ferrocifen Type Anti Cancer Drugs. *Chem Soc Rev* **2015**, *44* (24), 8802–8817. https://doi.org/10.1039/c5cs00486a.

(12) Top, S.; Dauer, B.; Vaissermann, J.; Jaouen, G. Facile Route to Ferrocifen, 1-[4-(2-Dimethylaminoethoxy)]-1-(Phenyl-2-Ferrocenyl-but-1-Ene), First Organometallic Analogue of Tamoxifen, by the McMurry Reaction. *Journal of Organometallic Chemistry* **1997**, *541* (1), 355–361. https://doi.org/10.1016/S0022-328X(97)00086-7.

(13) Jaouen, G.; Top, S.; Vessières, A.; Leclercq, G.; Quivy, J.; Jin, L.; Croisy, A. The First Organometallic Antioestrogens and Their Antiproliferative Effects. *Comptes Rendus de l'Académie des Sciences - Series IIC - Chemistry* **2000**, *3* (2), 89–93. https://doi.org/10.1016/S1387-1609(00)00118-3.

(14) Hillard, E.; Vessières, A.; Le Bideau, F.; Plazuk, D.; Spera, D.; Huché, M.; Jaouen, G. A Series of Unconjugated Ferrocenyl Phenols: Prospects as Anticancer Agents. *ChemMedChem* **2006**, *1* (5), 551–559. https://doi.org/10.1002/cmdc.200500035.

(15) Wang, Y.; Pigeon, P.; Top, S.; McGlinchey, M. J.; Jaouen, G. Organometallic Antitumor Compounds: Ferrocifens as Precursors to Quinone Methides. *Angew. Chem. Int. Ed. Engl.* **2015**, *54* (35), 10230–10233. https://doi.org/10.1002/anie.201503048.

(16) Pigeon, P.; Wang, Y.; Top, S.; Najlaoui, F.; Garcia Alvarez, M. C.; Bignon, J.; McGlinchey, M. J.; Jaouen, G. A New Series of Succinimido-Ferrociphenols and Related Heterocyclic Species Induce Strong Antiproliferative Effects, Especially against Ovarian Cancer Cells Resistant to Cisplatin. *J. Med. Chem.* **2017**, *60* (20), 8358–8368. https://doi.org/10.1021/acs.jmedchem.7b00743.

(17) Wang, Y.; Pigeon, P.; Top, S.; Sanz García, J.; Troufflard, C.; Ciofini, I.; McGlinchey, M. J.; Jaouen, G. Atypical Lone Pair-π Interaction with Quinone Methides in a Series of Imido-Ferrociphenol Anticancer Drug Candidates. *Angew. Chem. Int. Ed. Engl.* **2019**, *58* (25), 8421–8425. https://doi.org/10.1002/anie.201902456.

(18) Hureaux, J.; Lagarce, F.; Gagnadoux, F.; Rousselet, M.-C.; Moal, V.; Urban, T.; Benoit, J.-P. Toxicological Study and Efficacy of Blank and Paclitaxel-Loaded Lipid Nanocapsules after i.v. Administration in Mice. *Pharm Res* **2010**, *27* (3), 421–430. https://doi.org/10.1007/s11095-009-0024-y.

(19) Allard, E.; Passirani, C.; Garcion, E.; Pigeon, P.; Vessières, A.; Jaouen, G.; Benoit, J.-P. Lipid Nanocapsules Loaded with an Organometallic Tamoxifen Derivative as a Novel Drug-Carrier System for Experimental Malignant Gliomas. *J Control Release* **2008**, *130* (2), 146–153. https://doi.org/10.1016/j.jconrel.2008.05.027.

(20) Lainé, A.-L.; Clavreul, A.; Rousseau, A.; Tétaud, C.; Vessieres, A.; Garcion, E.; Jaouen, G.; Aubert, L.; Guilbert, M.; Benoit, J.-P.; Toillon, R.-A.; Passirani, C. Inhibition of Ectopic Glioma Tumor Growth by a Potent Ferrocenyl Drug Loaded into Stealth Lipid Nanocapsules. *Nanomedicine* **2014**, *10* (8), 1667–1677. https://doi.org/10.1016/j.nano.2014.05.002.

(21) Karim, R.; Lepeltier, E.; Esnault, L.; Pigeon, P.; Lemaire, L.; Lépinoux-Chambaud, C.; Clere,

N.; Jaouen, G.; Eyer, J.; Piel, G.; Passirani, C. Enhanced and Preferential Internalization of Lipid Nanocapsules into Human Glioblastoma Cells: Effect of a Surface-Functionalizing NFL Peptide. *Nanoscale* **2018**, *10* (28), 13485–13501. https://doi.org/10.1039/c8nr02132e.

(22) Heurtault, B.; Saulnier, P.; Pech, B.; Proust, J.-E.; Benoit, J.-P. A Novel Phase Inversion-Based Process for the Preparation of Lipid Nanocarriers. *Pharm. Res.* **2002**, *19* (6), 875–880. https://doi.org/10.1023/a:1016121319668.

(23) Topin-Ruiz, S.; Mellinger, A.; Lepeltier, E.; Bourreau, C.; Fouillet, J.; Riou, J.; Jaouen, G.; Martin, L.; Passirani, C.; Clere, N. P722 Ferrocifen Loaded Lipid Nanocapsules Improve Survival of Murine Xenografted-Melanoma via a Potentiation of Apoptosis and an Activation of CD8+ T Lymphocytes. *Int J Pharm* **2021**, *593*, 120111. https://doi.org/10.1016/j.ijpharm.2020.120111.

(24) Najlaoui, F.; Busser, B.; Taïwe, G. S.; Pigeon, P.; Sturm, N.; Giovannini, D.; Marrakchi, N.; Rhouma, A.; Jaouen, G.; Gibaud, S.; De Waard, M. Succinimido-Ferrocidiphenol Complexed with Cyclodextrins Inhibits Glioblastoma Tumor Growth In Vitro and In Vivo without Noticeable Adverse Toxicity. *Molecules* **2022**, *27* (14), 4651. https://doi.org/10.3390/molecules27144651.

(25) Idlas, P.; Ladaycia, A.; Némati, F.; Lepeltier, E.; Pigeon, P.; Jaouen, G.; Decaudin, D.; Passirani, C. Ferrocifen Stealth LNCs and Conventional Chemotherapy: A Promising Combination against Multidrug-Resistant Ovarian Adenocarcinoma. *International Journal of Pharmaceutics* **2022**, *626*, 122164. https://doi.org/10.1016/j.ijpharm.2022.122164.

(26) Lainé, A.-L.; Adriaenssens, E.; Vessières, A.; Jaouen, G.; Corbet, C.; Desruelles, E.; Pigeon, P.; Toillon, R.-A.; Passirani, C. The in Vivo Performance of Ferrocenyl Tamoxifen Lipid Nanocapsules in Xenografted Triple Negative Breast Cancer. *Biomaterials* **2013**, *34* (28), 6949–6956. https://doi.org/10.1016/j.biomaterials.2013.05.065.

(27) Huynh, N. T.; Morille, M.; Bejaud, J.; Legras, P.; Vessieres, A.; Jaouen, G.; Benoit, J.-P.; Passirani, C. Treatment of 9L Gliosarcoma in Rats by Ferrociphenol-Loaded Lipid Nanocapsules Based on a Passive Targeting Strategy via the EPR Effect. *Pharm. Res.* **2011**, *28* (12), 3189–3198. https://doi.org/10.1007/s11095-011-0501-y.

(28) Allard, E.; Jarnet, D.; Vessières, A.; Vinchon-Petit, S.; Jaouen, G.; Benoit, J.-P.; Passirani, C. Local Delivery of Ferrociphenol Lipid Nanocapsules Followed by External Radiotherapy as a Synergistic Treatment against Intracranial 9L Glioma Xenograft. *Pharm. Res.* **2010**, *27* (1), 56–64. https://doi.org/10.1007/s11095-009-0006-0.

(29) Almdal, K.; Dyre, J.; Hvidt, S.; Kramer, O. Towards a Phenomenological Definition of the Term 'Gel.' *Polymer Gels and Networks* **1993**, *1* (1), 5–17. https://doi.org/10.1016/0966-7822(93)90020-I.

(30) Moysan, E.; González-Fernández, Y.; Lautram, N.; Béjaud, J.; Bastiat, G.; Benoit, J.-P. An Innovative Hydrogel of Gemcitabine-Loaded Lipid Nanocapsules: When the Drug Is a Key Player of the Nanomedicine Structure. *Soft Matter* **2014**, *10* (11), 1767–1777. https://doi.org/10.1039/c3sm52781f.

(31) Pitorre, M.; Gazaille, C.; Pham, L. T. T.; Frankova, K.; Béjaud, J.; Lautram, N.; Riou, J.; Perrot, R.; Geneviève, F.; Moal, V.; Benoit, J.-P.; Bastiat, G. Polymer-Free Hydrogel Made of Lipid Nanocapsules, as a Local Drug Delivery Platform. *Materials Science and Engineering: C* **2021**, *126*, 112188. https://doi.org/10.1016/j.msec.2021.112188.

(32) Huynh, N. T.; Passirani, C.; Allard-Vannier, E.; Lemaire, L.; Roux, J.; Garcion, E.; Vessieres, A.; Benoit, J.-P. Administration-Dependent Efficacy of Ferrociphenol Lipid Nanocapsules for the Treatment of Intracranial 9L Rat Gliosarcoma. *Int J Pharm* **2012**, *423* (1), 55–62.

https://doi.org/10.1016/j.ijpharm.2011.04.037.

(33) Laine, A.-L.; Huynh, N. T.; Clavreul, A.; Balzeau, J.; Béjaud, J.; Vessieres, A.; Benoit, J.-P.; Eyer, J.; Passirani, C. Brain Tumour Targeting Strategies via Coated Ferrociphenol Lipid Nanocapsules. *Eur J Pharm Biopharm* **2012**, *81* (3), 690–693. https://doi.org/10.1016/j.ejpb.2012.04.012.

(34) Bastiancich, C.; Vanvarenberg, K.; Ucakar, B.; Pitorre, M.; Bastiat, G.; Lagarce, F.; Préat, V.; Danhier, F. Lauroyl-Gemcitabine-Loaded Lipid Nanocapsule Hydrogel for the Treatment of Glioblastoma. *Journal of Controlled Release* **2016**, *225*, 283–293. https://doi.org/10.1016/j.jconrel.2016.01.054.

(35) Bastiancich, C.; Lemaire, L.; Bianco, J.; Franconi, F.; Danhier, F.; Préat, V.; Bastiat, G.; Lagarce, F. Evaluation of Lauroyl-Gemcitabine-Loaded Hydrogel Efficacy in Glioblastoma Rat Models. *Nanomedicine (Lond)* **2018**, *13* (16), 1999–2013. https://doi.org/10.2217/nnm-2018-0057.

(36) Bastiancich, C.; Bozzato, E.; Luyten, U.; Danhier, F.; Bastiat, G.; Préat, V. Drug Combination Using an Injectable Nanomedicine Hydrogel for Glioblastoma Treatment. *Int J Pharm* **2019**, *559*, 220–227. https://doi.org/10.1016/j.ijpharm.2019.01.042.

(37) Vessières, A.; Quissac, E.; Lemaire, N.; Alentorn, A.; Domeracka, P.; Pigeon, P.; Sanson, M.; Idbaih, A.; Verreault, M. Heterogeneity of Response to Iron-Based Metallodrugs in Glioblastoma Is Associated with Differences in Chemical Structures and Driven by FAS Expression Dynamics and Transcriptomic Subtypes. *Int J Mol Sci* **2021**, *22* (19), 10404. https://doi.org/10.3390/ijms221910404.

(38) Najlaoui, F.; Pigeon, P.; Aroui, S.; Pezet, M.; Sancey, L.; Marrakchi, N.; Rhouma, A.; Jaouen, G.; De Waard, M.; Busser, B.; Gibaud, S. Anticancer Properties of Lipid and Poly(ε-Caprolactone) Nanocapsules Loaded with Ferrocenyl-Tamoxifen Derivatives. *J. Pharm. Pharmacol.* **2018**, *70* (11), 1474–1484. https://doi.org/10.1111/jphp.12998.

(39) Allard, E.; Huynh, N. T.; Vessières, A.; Pigeon, P.; Jaouen, G.; Benoit, J.-P.; Passirani, C. Dose Effect Activity of Ferrocifen-Loaded Lipid Nanocapsules on a 9L-Glioma Model. *Int J Pharm* **2009**, *379* (2), 317–323. https://doi.org/10.1016/j.ijpharm.2009.05.031.

(40) Wang, Y.; Pigeon, P.; McGlinchey, M. J.; Top, S.; Jaouen, G. Synthesis and Antiproliferative Evaluation of Novel Hydroxypropyl-Ferrociphenol Derivatives, Resulting from the Modification of Hydroxyl Groups. *Journal of Organometallic Chemistry* **2017**, *829*, 108–115. https://doi.org/10.1016/j.jorganchem.2016.09.005.

(41) Berry, J. D.; Neeson, M. J.; Dagastine, R. R.; Chan, D. Y. C.; Tabor, R. F. Measurement of Surface and Interfacial Tension Using Pendant Drop Tensiometry. *J Colloid Interface Sci* **2015**, *454*, 226–237. https://doi.org/10.1016/j.jcis.2015.05.012.

(42) Mouzouvi, C. R. A.; Umerska, A.; Bigot, A. K.; Saulnier, P. Surface Active Properties of Lipid Nanocapsules. *PLoS One* **2017**, *12* (8), e0179211. https://doi.org/10.1371/journal.pone.0179211.

(43) Xu, H.; Deng, Y.; Chen, D.; Hong, W.; Lu, Y.; Dong, X. Esterase-Catalyzed DePEGylation of PH-Sensitive Vesicles Modified with Cleavable PEG-Lipid Derivatives. *Journal of Controlled Release* **2008**, *130* (3), 238–245. https://doi.org/10.1016/j.jconrel.2008.05.009.

(44) Howard, M. D.; Lu, X.; Rinehart, J. J.; Jay, M.; Dziubla, T. D. Carboxylesterase-Triggered Hydrolysis of Nanoparticle PEGylating Agents. *Langmuir* **2012**, *28* (33), 12030–12037. https://doi.org/10.1021/la302144r.

(45) Vessières, A.; Wang, Y.; McGlinchey, M. J.; Jaouen, G. Multifaceted Chemical Behaviour of Metallocene (M = Fe, Os) Quinone Methides. Their Contribution to Biology. *Coordination Chemistry*

Reviews **2021**, *430*, 213658. https://doi.org/10.1016/j.ccr.2020.213658.

(46) Pitorre, M.; Gondé, H.; Haury, C.; Messous, M.; Poilane, J.; Boudaud, D.; Kanber, E.; Rossemond Ndombina, G. A.; Benoit, J.-P.; Bastiat, G. Recent Advances in Nanocarrier-Loaded Gels: Which Drug Delivery Technologies against Which Diseases? *J Control Release* **2017**, *266*, 140–155. https://doi.org/10.1016/j.jconrel.2017.09.031.

(47) Resnier, P.; Galopin, N.; Sibiril, Y.; Clavreul, A.; Cayon, J.; Briganti, A.; Legras, P.; Vessières, A.; Montier, T.; Jaouen, G.; Benoit, J.-P.; Passirani, C. Efficient Ferrocifen Anticancer Drug and Bcl-2 Gene Therapy Using Lipid Nanocapsules on Human Melanoma Xenograft in Mouse. *Pharmacol. Res.* **2017**, *126*, 54–65. https://doi.org/10.1016/j.phrs.2017.01.031.

(48) Bruyère, C.; Mathieu, V.; Vessières, A.; Pigeon, P.; Top, S.; Jaouen, G.; Kiss, R. Ferrocifen Derivatives That Induce Senescence in Cancer Cells: Selected Examples. *J. Inorg. Biochem.* **2014**, *141*, 144–151. https://doi.org/10.1016/j.jinorgbio.2014.08.015.

(49) Heilmann, J. B.; Hillard, E. A.; Plamont, M.-A.; Pigeon, P.; Bolte, M.; Jaouen, G.; Vessières, A. Ferrocenyl Compounds Possessing Protected Phenol and Thiophenol Groups: Synthesis, X-Ray Structure, and in Vitro Biological Effects against Breast Cancer. *Journal of Organometallic Chemistry* **2008**, *693* (8), 1716–1722. https://doi.org/10.1016/j.jorganchem.2007.12.011.

TOC Graphic

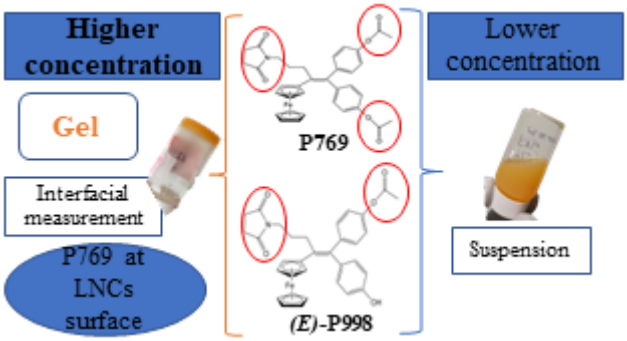
Higher concentration
Gel
Interfacial measurement
P769 at LNCs surface
P769
(E)-P998
Lower concentration
Suspension